One Electron Oxidation Induced Dimerization of 5-Hydroxytryptophol: Role of 5-Hydroxy Substitution

G. H. Naik, K. Indira Priyadarsini,* D. K. Maity, and Hari Mohan

Radiation Chemistry & Chemical Dynamics Division, Bhabha Atomic Research Centre,
Trombay, Mumbai-400085, India

Received: April 28, 2004; In Final Form: January 10, 2005

Reaction of one-electron oxidant ($Br_2^{\bullet -}$) with tryptophol (TP) and 5-hydroxytryptophol (HTP) have been studied in aqueous solution in the pH range from 3 to 10, employing nanosecond pulse radiolysis technique and the transients detected by kinetic spectrophotometry. One-electron oxidation of TP has produced an indolyl radical that absorbs in the 300−600 nm region with radical $pK_a = 4.9 \pm 0.2$, while the reaction with HTP has produced an indoloxyl radical with λ_{max} at 420 nm and radical $pK_a < 3$. Hydroxyl radicals ($^{\bullet}OH$) react with these two compounds producing $^{\bullet}OH$ radical adducts that undergo water elimination to give one-electron-oxidized indolyl and indoloxyl radical species, respectively. The indoloxyl radicals react with the parent compound to form dimer radicals with an average association constant of $(6.7 \pm 0.4) \times 10^4$ M^{-1}. No such dimerization is observed with indolyl radical, indicating that the presence of the 5-hydroxy group markedly alters its ability to form a dimer. A possible explanation behind such a difference in reactivity has been supported with ab initio quantum chemical calculations.

Introduction

Indoles are aromatic compounds found widely in nature. The oxidation chemistry of hydroxy-substituted indoles has been the subject of great interest due to their role in processes such as those for melanoma, antioxidant activity, and neurotransmission.[1−6] 5-Hydroxytryptophol is an indolic derivative produced during the metabolism of indole amine, serotonin, an important chemical neurotransmitter found in the central nervous system. These compounds are considered to be involved in the regulation of body temperature, sleep, pituitary function, etc.[3,4] Serotonin's nonhydroxylated analogue, tryptophol, has also been reported to be found in the brains of some experimental animals, although it may not play any role in neurotransmission.[5,7] Tryptophol is also found in several plants and wines.[8−10] It is considered to be a phytotoxin, and some reports indicate that tryptophol can cause scission in DNA.[10−12] It has been reported that the oxidized, hydroxylated, and dimeric products of neurotransmitters and their metabolites can act as neurotoxins in the human brain, and ultimately cause mental disorders.[2,13] Oxidative damage is a process often mediated by the reactive oxygen free radicals produced during biochemical processes.[1] To understand the effect of oxidation or oxidative stress on these compounds, it is necessary to understand the oxidation chemistry in detail and also to understand the role of the 5-hydroxy group in the overall oxidation reactions. For this, studies have been made with two indolic anlogues, 5-hydroxy-substituted indole and its nonhydroxylated analogue. There are some reports in the literature showing oxidation reactions of hydroxylated indolic compounds. Dryhurst et al. have studied the electrochemical oxidation of indolic neurotransmitters and their metabolites, where a number of products have also been isolated and characterized.[3,4,13−15] The mechanism and free radical reactions involved in the oxidation of substituted indolic compounds have been studied using flash photolysis and pulse radiolysis techniques.[16−23] Using these techniques, the spectral, redox, and acid−base properties of several substituted indoles have been reported.[16−21] Pulse radiolysis technique is a very convenient and versatile tool, where the reactions of many oxidizing radicals can be monitored selectively in very short time scales (less than microseconds).[16−23] Pulse radiolysis studies on the hydroxyl radical induced oxidation chemistry of serotonin and tryptamine have been reported by us earlier.[16] In this paper, we present reactions of hydroxyl radicals (one of the most important and reactive oxygen free radicals) with tryptophol (TP) and 5-hydroxytryptophol (HTP) at different pH conditions using nanosecond pulse radiolysis. To understand the oxidation chemistry, studies have also been made with some specific one-electron oxidants. To assign the structure and nature of the bonding of the transient species, we have used ab initio quantum chemical methods.[24] The chemical structures of these compounds are given in Scheme 1.

Experimental Section

Materials. Tryptophol (TP) and 5-hydroxytryptophol (HTP) were obtained from Sigma Chemicals and used without further purification. All other chemicals and reagents were of AnalaR grade and used as such. Solutions were prepared in Nanopure water obtained from a Barnstead Nanopure water purification system, and freshly prepared solutions were used for each experiment. The pH of the solutions was adjusted using $HClO_4$, Na_2HPO_4, KH_2PO_4, and NaOH. N_2 and N_2O gases used were of IOLAR grade purity and were obtained from Indian Oxygen Ltd., Mumbai, India.

Pulse Radiolysis Studies. Pulse radiolysis experiments were carried out with high energy electron pulses (7 MeV, 50 ns) obtained from a linear electron accelerator, and the transient species were detected by an optical absorption detection

---

* To whom correspondence should be addressed. E-mail: kindira@apsara.barc.ernet.in.

10.1021/jp048157r CCC: $30.25

SCHEME 1 : Chemical Structures of TP and HTP

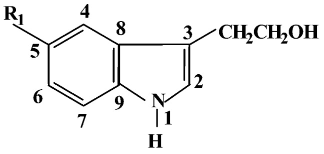

R_1 = -H Tryptophol (TP)

R_1 = -OH 5-Hydroxy Tryptophol (HTP)

technique whose details are given elsewhere.[25] Aerated aqueous solution of KSCN (0.01 M) was used to measure the absorbed dose.[26] The typical dose per pulse was kept close to 12−15 Gy (1 Gy = 1 J kg^{-1}). Wherever required, the experiments were carried out at a higher dose of 35 Gy per pulse. The absorption−time signals were analyzed for first- or second-order kinetics, and the rate constant values were taken from that kinetic analysis for which very good overlay was obtained between the experimental and the calculated fitted curve. The bimolecular rate constant was determined from the linear regression plot of k_{obs} versus solute concentration for at least three experiments, and the variation was within ±10%.

Hydroxyl radicals were generated by the radiolysis of N_2O-saturated water, where e_{aq}^- is converted into $^\bullet$OH radicals, giving the radiation chemical yield of 0.56 μmol J^{-1}. The one-electron oxidants $Br_2^{\bullet-}$ and $N_3^\bullet$ radicals were generated by radiolysis of N_2O-saturated aqueous solutions containing 0.02 M KBr and 0.02 M NaN_3, respectively, with radiation chemical yields close to 0.6 μmol J^{-1}. Corrections in radiation chemical yields were made whenever higher concentrations of these substrates are used. The details regarding the generation of different oxidizing radicals by radiolysis are given in the literature.[27,28]

Theoretical Studies. Full geometry optimizations were performed to predict the most stable structures of TP and HTP, their radical cations, namely, indolyl radical and indoloxyl radical, respectively, under gas phase isolated condition at the B3LYP level of theory with the 6-31+G(d,p) set of basis functions. B3LYP is a correlated density functional and is very popular for giving reasonably accurate geometry. The optimized gas phase molecular geometry was reoptimized fully including solvent effects following the Onsager reaction field model with the cavity radius based on gas phase optimized geometry. A Hessian calculation was also done at the same level of theory to check the nature of the stationary geometry. Calculations were also performed for different dimer radicals at the same level of theory and basis functions. The total number of Cartesian Gaussian functions for each dimer radical systems was 536. The initial guess geometry for dimer radical systems was obtained on the basis of semiempirical geometry optimizations at the PM3 level. All these calculations were performed adopting the GAMESS suite of programs on a PC-based LINUX cluster platform.[24]

Results and Discussion

One-Electron Oxidation Studies. *Reaction with $Br_2^{\bullet-}$.* The transient absorption spectra obtained 20 μs after the pulse, on reaction of $Br_2^{\bullet-}$ with 200 μM TP at pH 3 and 9, are shown in Figure 1a and 1b, respectively. Time-resolved studies confirmed that the $Br_2^{\bullet-}$ radicals absorbing at 360 nm decayed completely by this time, and the spectrum represents the transient spectra of one-electron-oxidized TP only. A similar spectrum was observed on reaction of TP with another oxidizing radical, $N_3^\bullet$ (results not shown). The transient spectrum shows two absorption peaks: one in the 320−330 nm region and another in the 500−600 nm region. The absorption in the 500 nm region showed significant changes with the pH of the solution (Figure 1a,b), indicating the presence of prototropic equilibrium in this pH range. The absorbance values at 570 and 480 nm were followed as a function of pH (inset c of Figure 1), and the pK_a of the one-electron-oxidized radicals of tryptophol was determined to be 4.9. The radical pK_a and the transient spectra of TP indicate the formation of indolyl radicals (II, Scheme 2) as similar results were reported in the cases of tryptamine, tryptophan, methylindoles, and methoxyindoles, and the radical pK_a has been attributed to the prototropic equilibrium at the N(1) position.[16−22] The nature of the spectrum at all pH values remained unaffected with the presence of oxygen, indicating that the indolyl radicals do not react with oxygen. The bimolecular rate constant for the reaction of $Br_2^{\bullet-}$ radical with TP at pH 7 was determined to be 1.6 × 10^9 M^{-1} s^{-1} by following the decay of $Br_2^{\bullet-}$ radicals at 360 nm in the presence of various concentrations of TP (20−100 μM) and from the slope of the linear plot of the pseudo-first-order rate constant (k_{obs}) as a function of TP concentration. This bimolecular rate constant did not change significantly with the pH of the solution.

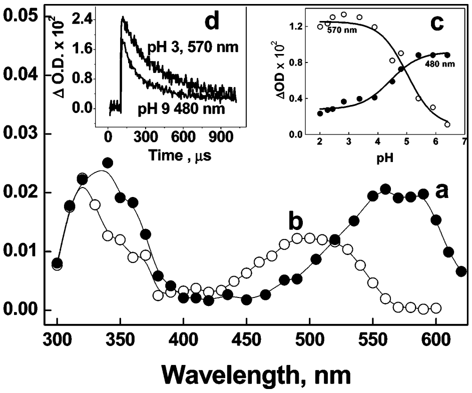

Figure 1. Difference transient absorption spectra recorded 20 μs after pulse, obtained on pulse radiolysis of N_2O-saturated aqueous solutions of tryptophol (200 μM) containing KBr (0.02 M) at (a) pH 3 and (b) pH 9 (dose per pulse = 14.7 Gy). Inset c shows variation in the absorbance at 480 and 570 nm as a function of pH under similar experimental conditions (dose per pulse = 13.1 Gy). Inset d gives the absorption−time plots for the decay of TP radical at 580 and 470 nm at pH 3 and 9 respectively under similar experimental conditions (dose per pulse = 34.4 Gy).

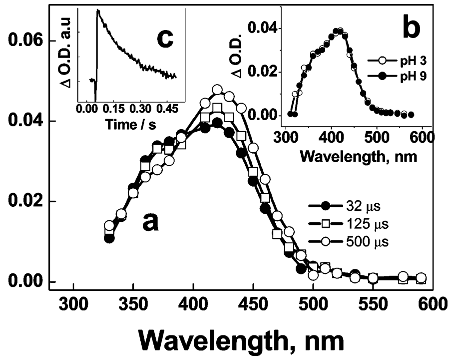

Figure 2. (a) Time-resolved absorption spectra of transients produced on pulse radiolysis of N_2O-saturated aqueous solutions (pH 7) containing HTP (100 μM) and KBr (0.02 M) at (●) 32 μs, (□) 125 μs, and (○) 500 μs after pulse (dose per pulse = 14.9 Gy). Inset b shows difference transient absorption spectra recorded at 40 μs after pulse under similar experimental conditions at (○) pH 3 and (●) pH 9 (dose per pulse = 14.3 Gy). Inset c shows absorption−time plot with decay of dimer radical at 420 nm, generated by pulse radiolysis of N_2O-saturated aqueous solutions containing 1 mM HTP, 0.1 M KBr at pH 7 (dose per pulse = 30 Gy).

SCHEME 2: Mechanism of One-Electron Oxidation of TP and HTP

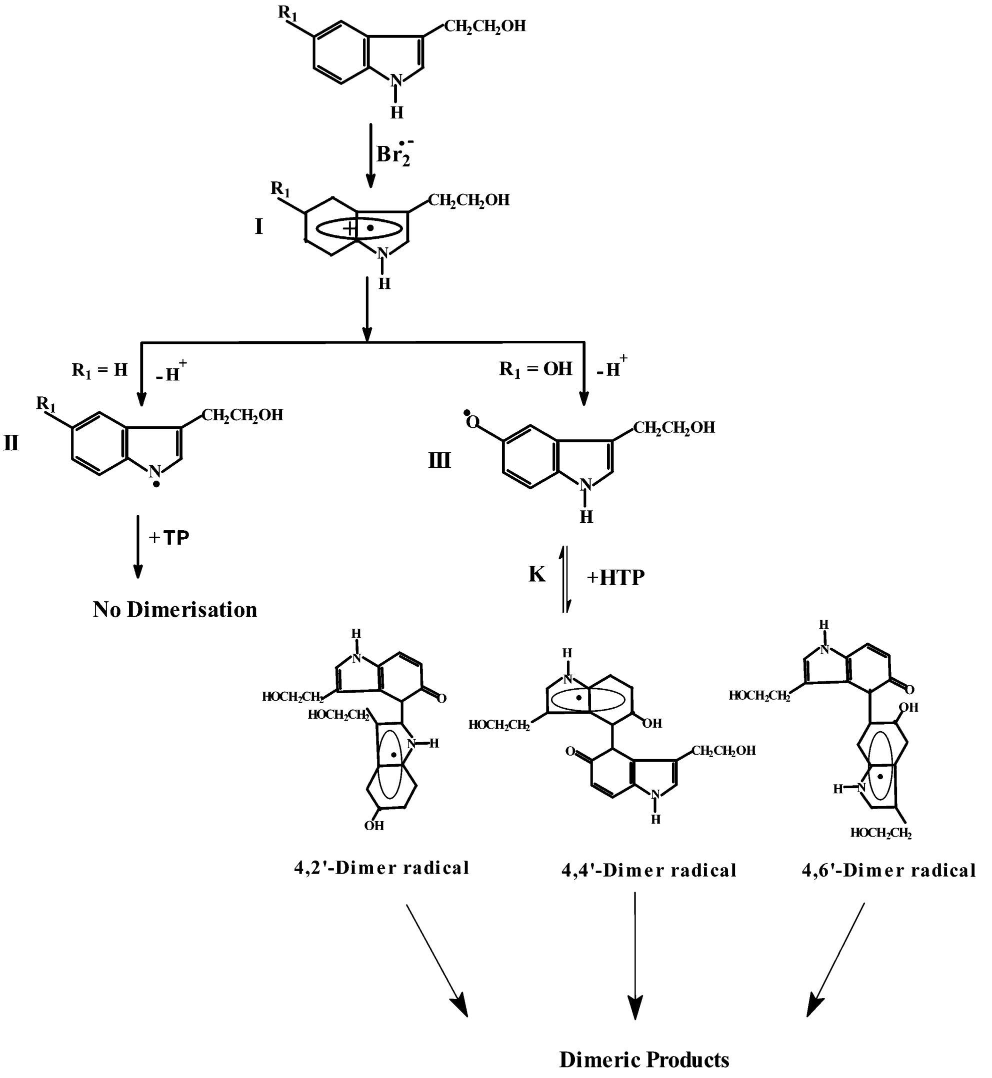

The indolyl radicals decay by second-order kinetics, indicating radical−radical reactions with a 2*k* value of 5.8×10^8 dm^3 mol^{-1} s^{-1}. The decay traces at pH 3 and pH 9 at 570 and 480 nm, respectively, are given as inset d of Figure 1.

Reaction of $Br_2^{\bullet-}$ with 200 μM HTP produced a transient absorption spectrum in the 300−500 nm region with maximum absorption at 420 nm at pH 7 (Figure 2a, 32 μs after the pulse). This spectrum was found to be independent of pH from pH 3 to 9 (Figure 2b). The spectrum looked significantly different from that obtained on reaction of $Br_2^{\bullet-}$ with TP (Figure 1). The presence of a 5-hydroxy group has changed the nature of the one-electron-oxidation process. The absorption band at 420 nm is characteristic of the indoloxyl radical (III, Scheme 2), which is produced by the one-electron oxidation followed by deprotonation at the OH group. Assignment of the spectrum (Figure 2a) to the indoloxyl radicals is analogous to that reported for serotonin and other 5-hydroxyindoles.[16,21] In general, the phenoxyl-type indoloxyl radicals have p$K_a \ll 3$ and hence do not change in this pH range. Like the indolyl radicals, the indoloxyl radicals also did not show any reaction with oxygen.

Careful examination of reaction of $Br_2^{\bullet-}$ radicals with HTP revealed that the one-electron-oxidation reaction is a complex process and is different at different concentrations of HTP involving multiple reactions. Following the decay kinetics of $Br_2^{\bullet-}$ radicals at 360 nm and formation kinetics of HTP radicals at 420 nm in the presence of 200 μM HTP, it was observed that although the decay of $Br_2^{\bullet-}$ radicals and the initial one-electron transfer is complete in <20 μs, the absorption at 420 nm continuously increases even after the reaction is over (Figure 2a, transient spectra recorded at 125 and 500 μs after the pulse). This suggests that the initially formed indoloxyl radicals of HTP undergo further reactions and therefore have been examined in detail.

The rate of this slowly rising species was found to depend on the concentration of HTP. Figure 3 gives the transient spectrum obtained at 450 μs after the pulse on reaction of $Br_2^{\bullet-}$ radicals with HTP at 50 and 1000 μM concentrations. The absorption−time plots at 420 nm at HTP concentrations in the range from 50 to 400 μM are given as the inset of Figure 3. From this figure, it can be seen that the absorption spectra of the transients produced at low and high HTP concentrations are qualitatively similar and only the absorbance at 420 nm increased with increasing HTP concentration. Such spectral overlap and increase in absorbance with increasing concentration have been observed earlier in several cases[29,30] and explained on the basis of conversion of the monomer radicals into dimer radicals on reaction with excess parent. Therefore, there is a possibility of the existence of an equilibrium between the monomer and dimer radicals (Scheme 2). According to the procedure given in refs 29 and 30 and using this change in absorbance at 420 nm as a function of HTP concentration, the

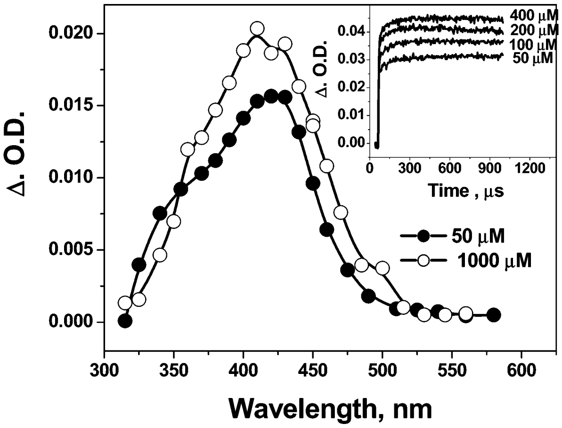

Figure 3. Difference absorption spectra of transient recorded at 500 μs after pulse generated by pulse radiolysis of N_2O-saturated aqueous solutions of 0.1 M KBr, at pH 7 containing (●) 50 μM and (○) 1 mM HTP (dose per pulse = 6.1 Gy). Inset shows absorption−time plots at 420 nm generated by pulse radiolysis of N_2O-saturated aqueous solutions at pH 7 containing 0.02 M KBr and different concentrations of HTP (dose per pulse = 13.5 Gy).

association constant (*K*) for the formation of dimer radical is determined by

$$\frac{A_0}{A} = 1 + K^{-1}[\mathrm{HTP}]^{-1} \qquad (1)$$

Here A_0 and A are the transient absorbances at the maximum of the absorption−time plot at 420 nm for aqueous solution of HTP at pH 7 containing 1 mM and any other known concentration of HTP in the concentration range from 50 μM to 1 mM, respectively. The plot of A_0/A against the reciprocal concentration of [HTP] gave a straight line with the intercept value of 1, and from the slope the association constant (*K*) was evaluated to be $(6.7 \pm 0.4) \times 10^4$ M^{-1}. This value corresponds to an average value of *K* for all possible dimerization reactions. This value indicates a strong possibility for the dimerization.

From the inset of Figure 3, it can be seen that not only is there a slowly rising component increasing with increasing parent concentration, but the initial absorbance also increases. This suggests that the initially formed indoloxyl radicals react with the parent (HTP), by multiple reactions that may produce different kinds of dimers. Dryhurst et al. identified the formation of different types of dimers and some trimers using electrochemical oxidation of hydroxyindoles.[2−4] According to them the dimerization can take place either through the oxygen atom of indoloxyl radicals or through the radical site at 2(C), 3(C), 4(C), 6(C), or 1(N). A dimer can also be formed by the recombination of two indoloxyl radicals. At the concentration of radicals produced by pulse radiolysis, radical−parent reactions always predominate over the radical−radical recombinations. In the case of HTP they have reported three major dimer products 4,4′, 4,2′, and 4,6′ and further studies showed formation of several other dimers and trimers.[3,4] Blanchard et al. by radiolytic oxidation of HTP have observed a number of uncharacterized products and identified formation of a 4,4′-dimer as one of the products.[23]

The dimer radical of HTP absorbing at 420 nm was found to decay by first-order kinetics with *k* of 7.0 ± 0.5 s^{-1} (inset c of Figure 2), indicating that the radical decays by intramolecular rearrangement to give products. However, such reactions were not observed with TP, where the indolyl radicals, produced by one-electron oxidation, undergo second-order decay to give products. All these reactions are summarized in Scheme 2.

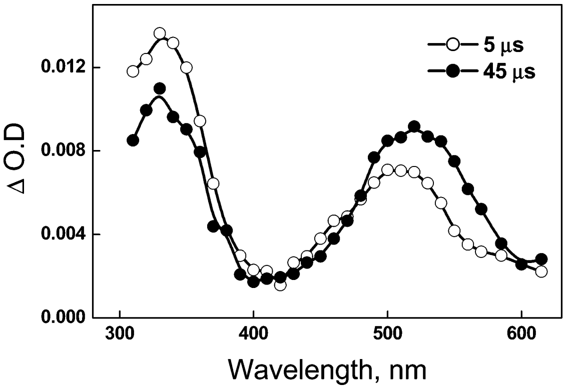

Figure 4. (a) Time-resolved spectra showing transformation of hydroxyl radical adduct of TP to indolyl radical produced on pulse radiolysis of N_2O-saturated aqueous solutions containing 100 μM TP at pH 9 (○) 5 μs and (●) 45 μs after pulse (dose per pulse = 10.2 Gy).

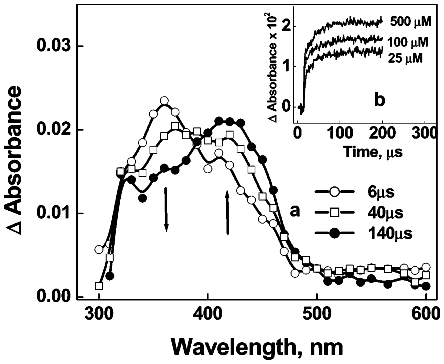

Figure 5. (a) Time-resolved spectra showing decay of hydroxyl radical adduct of HTP to form indoloxyl radicals produced, on pulse radiolysis of N_2O-saturated aqueous solutions containing 100 μM HTP at pH 7 recorded at (○) 6 μs, (□) 40 μs, and (●) 140 μs after pulse (dose per pulse = 14.8 Gy). Inset b shows absorption−time plots at 420 nm generated by pulse radiolysis of N_2O-saturated aqueous solutions at pH 7 containing different concentrations of HTP (dose per pulse = 12 Gy).

Reaction with $^{\bullet}$*OH Radicals.* The transient spectra produced on reaction of $^{\bullet}$OH radical with 100 μM TP and HTP at pH 7 are shown in Figures 4 and 5, respectively. The rate constants for these reactions are within the diffusion-controlled limit. The spectra recorded at 5 μs after the pulse (Figure 4 and Figure 5a) look different from those obtained on reaction of $Br_2^{\bullet -}$ with TP (Figure 1) and HTP (Figure 2), suggesting that the reaction proceeds by processes other than one-electron oxidation alone. It is known that $^{\bullet}$OH radicals react by different ways, such as addition to the aromatic ring forming radical adducts, one-electron oxidation, and hydrogen abstraction processes.[27,28] All three processes may take place with these compounds. Earlier it was reported that the hydroxyl radical adducts of several substituted indoles undergo water elimination, to finally yield one-electron-oxidized species.[16,22] In the present studies too, such a reaction was observed with TP and HTP. The spectra after 5 μs in Figures 4 and 5a correspond to the initial reaction of OH radicals with TP and HTP, respectively. The absorption peak in the 300 nm region may have a large contribution from the radical adduct, while the absorption in 400−600 nm corresponds to the one-electron-oxidized species, indicating that the reaction produces both radical adducts and one-electron-oxidized species. The spectra in Figures 4 and 5a after subsequent time points showed a decrease in the absorbance in the 300 nm region followed by a simultaneous increase in the formation of new transients having the absorption spectrum, which matches well with that of one-electron-oxidized species

SCHEME 3: Mechanism of Hydroxyl Radical Reaction of TP and HTP

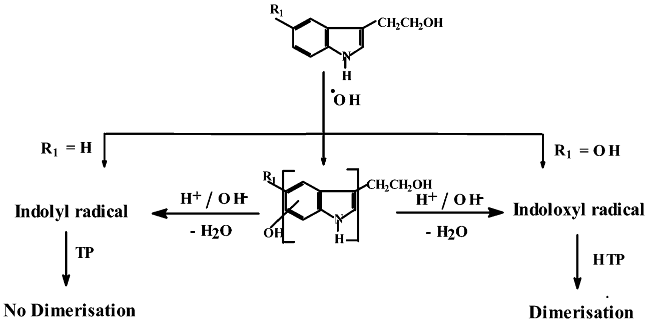

(Figure 1 and Figure 2, respectively) of TP and HTP. The rate of formation of the 520 or 420 nm signal obeyed first-order kinetics and did not depend on the parent concentration from 25 to 500 μM (inset b of Figure 5). However, in the case of HTP, the absorbance at 420 nm increased with increasing parent concentration, suggesting the possibility of dimerization reactions as observed with the $Br_2^{\bullet-}$ reaction.

The reaction of $^{\bullet}$OH radicals with TP has not shown any change in absorbance or change in spectrum with increasing TP concentration, suggesting that the dimerization process is not taking place even under hydroxyl radical reaction conditions. These reactions are summarized in Scheme 3.

On the basis of the above experimental studies, it has been concluded that hydroxyl radicals and one-electron oxidants react with tryptophol and 5-hydroxytryptophol to give indolyl radicals and indoxyl radicals, respectively. The indoloxyl radicals have a tendency to react with the parent and are converted to dimer radicals, while indolyl radicals do not indicate dimer formation under these experimental conditions, suggesting the requirement of oxygen centered radicals (indoloxyl radicals) for dimerizations. The present transient studies based on absorption technique do not show any evidence for the possible sites of dimerization. To understand this, we made theoretical calculations as discussed below.

Theoretical Studies. To determine the atomic charge distributions over different atoms in tryptophol (TP), 5-hydroxytryptophol (HTP), and their radicals in solution, molecular geometries were fully optimized including solvent effect, following Onsager's reaction field model. The fully optimized geometries of indolyl and indoloxyl radicals including solvent effect with spherical cavity radii of 4.39 and 4.35 Å, respectively, are shown in Figure 6A and Figure 6B, respectively. It is to be noted that Onsager's reaction field model does not consider true molecular shape. However, adopting a solvation model considering the molecular shape is beyond the scope at present as the systems are open-shell radicals and GAMESS cannot handle open-shell systems adopting a solvation model like COSMO (conductor like screening model) that considers molecular shape cavity. Neither Mulliken nor Löwdin atomic charge distributions show any indication for the observed change in reactivity to form dimers on adding a 5-hydroxy group in tryptophol. However, the calculated atomic spin population data in these two open-shell systems do show a proper trend in support of the observed change in reactivity in HTP. The calculated spin populations (Mulliken) ($\alpha-\beta$) over different atoms of these two radicals at B3LYP/6-31+G(d,p) level of theory are displayed in Table 1. As one can see, the odd electron spin is mostly populated over 3(C) and a small part over 1(N) in the case of indolyl radical. The presence of the 5-hydroxy group is thus observed to change the distribution of the spin population significantly. The major portion of the odd electron spin in indoxyl radical is now located on 4(C) and 14(O), indicating the high reactivity of these two sites. Thus, the radical species can react with the parent system either through the 4(C) site or the 14(O) site (see Figure 6). The large spin population on 4(C) explains the observed dimer product initiated through 4(C) in 5-hydroxytryptophol. In the case of indolyl radical, most of the spin population is localized over the 3(C) position and the position is sterically hindered to form dimeric products, thus explaining the experimental results. In principle, the 4(C) and 14(O) active sites of the indoloxyl radical can attack several sites of the parent system (HTP) with

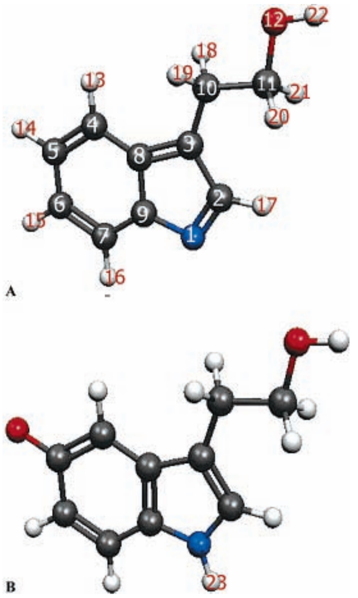

Figure 6. Optimized structure of indolyl (A) and indoloxyl (B) radical at correlated density functional theory (B3LYP) level with 6-31+G-(d,p) set of basis functions including solvent effect following Onsager's reaction field model. Black balls represent carbon atoms, gray balls represent hydrogen, blue balls represent nitrogen, and red balls represent oxygen.

TABLE 1: Atomic Spin Population ($\alpha-\beta$) over Different Atoms of Indolyl and Indoloxyl Radicals Calculated at B3LYP/6-31+G(d,p) Level of Theory in the Fully Optimized Structures at the Same Level of Theory Including Solvent Effect

	Mulliken spin population ($\alpha-\beta$)	
atom	indolyl radical	indoloxyl radical
1N	0.203	0.094
2C	0.045	−0.052
3C	0.435	0.115
4C	0.096	0.357
5C	0.016	0.012
6C	0.072	0.165
7C	0.038	−0.046
8C	0.040	−0.118
9C	0.009	0.161
10C	0.006	−0.017
11C	0.001	0.001
12O	0.002	−0.000
13H	0.000	−0.016
14H/O	0.000	0.346
15H	0.000	−0.008
16H	0.000	0.001
17H	0.000	0.002
18H	0.018	0.004
19H	0.000	0.004
20H	0.000	−0.000
21H	0.000	−0.000
22H	0.000	−0.000
23H		−0.005

SCHEME 4: Possible Reactions of Indoloxyl Radical (R = CH_2CH_2OH)

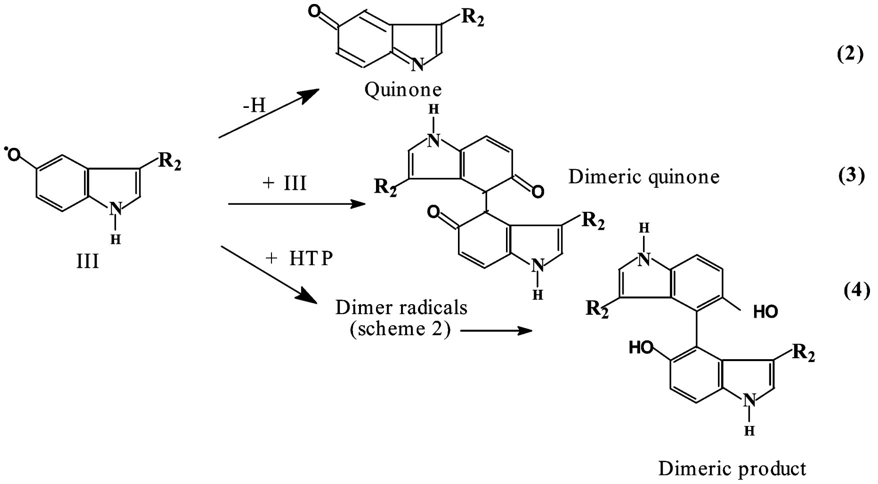

a preference for a few sites. As a result, a large number of transient dimer radical systems will be generated. However, the possible dimer radical systems are very large in size (47 atoms) for ab intio molecular structure calculations with large size basis functions (536 Cartesian basis functions for 6-31+G** basis functions). Thus, at present we have restricted ourselves to three dimer (4,2′, 4,4′, and 4,6′ linked) radical systems that have been reported by electrochemical oxidation, as discussed in the previous section[3,4] for theoretical calculations.

The fully optimized structures for all three dimer radical systems at the B3LYP/6-31+G(d,p) level of theory are displayed in Figure 7. The initial guess geometries for these calculations were carried out at the semiempirical PM3 level. Several conformers for each dimer radical were tried at PM3 level geometry optimization to determine the most stable structure of each dimer radical system in the gas phase isolated condition. The most stable PM3 structure was then reoptimized at the B3LYP/6-31+G(d,p) level to find the structure and the relative stability of the dimer radicals. The 4,2′ dimer radical system was predicted to be the most stable of these three radical systems studied at present. The 4,6′ dimer radical system was found to be less stable by 0.5 kcal/mol compared to 4,2′, while 4,4′ was found to be least stable by 4.5 kcal/mol. Although the difference in their stability is very small, inclusion of a suitable solvent model may alter this trend and explain why 4,4′ has been considered to be the most abundant dimer product. A detailed followup is required to clarify these aspects, which is planned in the near future.

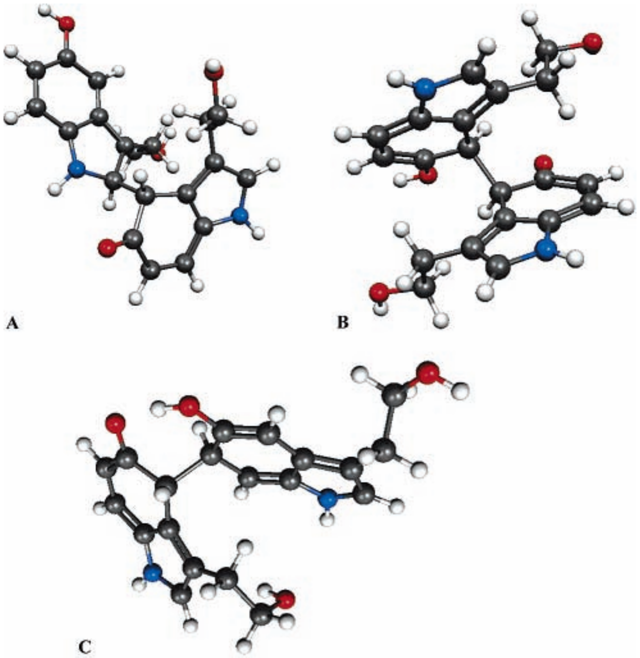

Figure 7. Optimized structure for radicals of 4,2′ (A), 4,4′ (B), and 4,6′ (C) dimers at correlated density functional theory (B3LYP) level with 6-31+G(d,p) set of basis functions in the gas phase. Black balls represent carbon atoms, gray balls represent hydrogen, blue balls represent nitrogen, and red balls represent oxygen.

To further support our hypothesis for the preferential conversion of indoloxyl radical to dimer radical, we made an attempt to estimate the energetics for all possible reactions of indoloxyl radicals with the same DFT functional. For this we considered three important reactions of indoloxyl radicals such as unimolecular radical conversion to products, radical−radical recombination leading to quinone dimers linked through 4,2′, 4,4′, and 4,6′ sites, and radical−parent reactions such as those given in Scheme 2. Other processes such as radical disproportionation are not considered. These three possible reactions are summarized in Scheme 4, with molecular structures shown for the 4,4′ product only.

It is predicted that reaction 2 is endothermic by 92.6 kcal/mol. Reaction 3 is predicted to be more endothermic than reaction 2 with respective energies of 154.4, 153.4, and 160.3 kcal/mol for the formation of 4,2′, 14,4′, and 14,6′ dimers. Reaction 4 is observed to be the least endothermic with relative energies of 42.3, 53.4, and 56.9 kcal/mol, respectively, for the formation of dimer radicals of 4,2′, 4,4′, and 4,6′ sites. Also, the subsequent reaction (reaction 3, Scheme 4) leading to the transformation of dimer radicals into corresponding dimer products is found to be exothermic by 7.2, 8.9, and 15.9 kcal/mol, respectively, for 4,2′, 4,4′, and 4,6′ sites. Comparing the energetics for these three reactions (reactions 2−4 in Scheme 4), it is clear that the indoloxyl radical prefers to form dimer radical through its parent reaction over the other processes. This supports our analysis and experimental observations, where dimerization of indoloxyl reaction through the parent reaction is the most preferred reaction in the case of 5-hydroxytryptophol.

Excited-state calculations were also carried out for the above three transient species at the semiempirical ZNDO level of theory on PM3 optimized gas phase geometry. These transients were predicted to absorb in the range of 370−380 nm with large oscillator strengths ($f \sim 0.36$). The dimer radical transients formed on 14(O) active site initiation were also calculated at the PM3 level. The geometry was fully optimized for several possible conformers on 14,2′, 14,4′, and 14,6′ linked dimer radical systems to determine the most stable conformer. Excited-state calculations were also carried out for these transient species at the ZNDO level of theory on PM3 optimized geometry. These transients were predicted to absorb at ∼300 nm with small oscillator strengths ($f \sim 0.02$). These semiempirical results suggest that the observed transient absorption peaks in the pulse radiolysis experiments are not due to 14(O) linked dimer radicals. Thus, the observed strong optical absorption band at ∼400 nm in the present pulse radiolysis experiments is due to a mixture of different dimer radical systems linked through the 4(C) site only.

Conclusions

Tryptophol (TP) and 5-hydroxytryptophol (HTP) react with one-electron oxidants such as $Br_2^{\bullet -}$ with diffusion-controlled rates to undergo electron transfer. The one-electron-oxidized species in the case of TP produces indolyl radicals with the radicals centered at indolyl nitrogen N(1), as determined by transient spectra, decay kinetics, and prototropic equilibria. The radical pK_a value of 4.9 determined for the TP radical is close to the values reported for many indolic derivatives. The indolyl radicals do not react with oxygen and decay by second-order reaction. The one-electron-oxidized species produced from HTP are significantly different from that of TP. The absence of pK_a in the range from 2.5 to 10 indicates that the transient is similar to the indoloxyl radicals observed during the oxidation of 5-hydroxyindoles.[16,21] The initially formed one-electron-oxidized species lose proton with $pK_a < 3$ to give a phenoxyl-type radical.

The indoloxyl radicals undergo further reaction with the parent molecule to give a dimer radical, which has a much longer lifetime (∼0.5 s) and shows no reaction with oxygen. Such dimeric species have been found to be the major products in electrochemical oxidations of 5-hydroxy-substituted indoles.[3,4] The pulse radiolysis studies therefore gave direct evidence for such dimerization process in the case of 5-hydroxyindoles. Such dimerization reactions are more prominent through the initiation of the 4(C) site of indoloxyl radical with the parent, yielding several dimer products linked by the 4(C) position as predicted by the present theoretical calculations. This dimerization reaction was not seen in the case of short-lived nitrogen centered indolyl radicals produced by oxidation of TP, thereby confirming that 5-hydroxy substitution plays an important role in the oxidative dimerization of substituted indoles.

Acknowledgment. The authors are thankful to Dr. T. Mukherjee, Head, Radiation Chemistry & Chemical Dynamics Division, for his support to this work. BARC Computer Centre is gratefully acknowledged for the computational facility.

References and Notes

(1) Bensasson, R. V.; Land, E. J.; Truscott, T. G. *Excited State and Free Radicals in Biology and Medicine*; Oxford University Press: Oxford, 1993; p 228.

(2) Wrona, M. Z.; Dryhurst, G. *Biochem. Pharmacol.* **1991**, *41*, 1145.

(3) Dryhurst, G. *Chem Rev.* **1990**, *90*, 795−811.

(4) Cheng, F. C.; Wrona, M. Z.; Dryhurst, G. *J. Electroanal. Chem.* **1991**, *310*, 187.

(5) Kveder, S.; Iskric, S.; Keglevic, D. *Biochemistry* **1962**, *85*, 447.

(6) Sono, M. *Biochemistry* **1989**, *28*, 5400.

(7) Yamada, J.; Sugimoto, Y.; Horisaka, K. *Anal. Biochem.* **1983**, *129*, 460.

(8) Lacan, G.; Magnus, V.; Simaga, S.; Iskric, S.; Hall, P. *J. Plant Physiol.* **1985**, *78*, 447.

(9) Gil, C.; Gomez-Cordoves, C. *Food Chem.* **1986**, *22*, 59.

(10) Sugawara, F.; Strobel, G. A. *Phytochemistry* **1987**, *26*, 1349.

(11) Tanaka, K.; Mcconnell, B.; Niemczura, W. P.; Mower, H. F. *Cancer Lett.* **1989**, 109.

(12) Fukumori, R.; Minegishi, A.; Satoh, T.; Kitagawa, H. *J. Pharm. Pharmacol.* **1981**, *33*, 586.

(13) Wrona, M. Z.; Goyal, R. N.; Turk, D. J.; Blank, C. L.; Dryhurst, G. *J. Neurochem.* **1992**, *59*, 1392.

(14) Biryol, I.; Ozkan, S.; Kabasakaloglu, M. *Electrochim. Acta* **1994**, *12*, 95.

(15) Wrona, M. Z.; Dryhurst, G. *J. Org. Chem.* **1987**, *52*, 2817.

(16) Hela, P. G.; Anipindi, N. R.; Priyadarsini, K. I.; O'Neill, P. *J. Phys. Chem.* **1999**, *103*, 8606.

(17) Jovanovic, S. V.; Steenken, S.; Simic, M. G. *J. Phys. Chem.* **1990**, *94*, 3583.

(18) Candeias, L. P.; Wardman, P.; Mason, R. P. *Biophys. Chem.* **1999**, *67*, 229.

(19) Al-Kazwini, A. T.; O'Neill, P.; Adams, G. E.; Cundall, R. B.; Junino, A.; Maignan, J. *J. Chem. Soc., Perkin Trans. 2* **1992**, 657.

(20) Shen, X.; Lind, J.; Merenyi, G. *J. Phys. Chem.* **1987**, *91*, 4403.

(21) Al-Kazwini, A. T.; O'Neill, P.; Adams, G. E.; Cundall, R. B.; Jacquet, B.; Lang, G.; Junino, A. *J. Phys. Chem.* **1990**, *94*, 6666.

(22) Naik, G. H.; Priyadarsini, K. I.; Mohan, H. *Res. Chem. Intermed.* **2003**, *29*, 641.

(23) Blanchard, B.; Dendane, M.; Gallard, J. F.; Levin, C, H.; Karim, A.; Payen, D.; Launay, J. M.; Ducrocq, C. *Nitric Oxide: Biol. Chem.* **1997**, *6*, 442.

(24) Schmidt, M. W.; Baldridge, K. K.; Boatz, J. A.; Elbert, S. T.; Gordon, M. S.; Jensen, J. H.; Koseki, S.; Matsunaga, N.; Nguyen, K. A.; Su, S. J.; Windus, T. L.; Dupuis, M.; Montgomery, J. A. *J. Comput. Chem.* **1993**, *14*, 1347.

(25) Guha, S. N.; Moorthy, P. N.; Kishore, K.; Naik, D. B.; Rao, K. N. *Proc. Indian Acad. Sci. (Chem. Sci.)* **1987**, *99*, 261.

(26) Fielden, F. M. In *The Study of Fast Processes and Transient Species by Electron Pulse Radiolysis*; Baxendale, J. H., Busi, F., Eds.; Reidel: Boston, 1982; p 59.

(27) Spinks, J. W., T.; Woods, R. J. In *An Introduction to Radiation Chemistry*; John Wiley: New York, 1990.

(28) von Sonntag, C. *The Chemical Basis of Radiation Biology*; Taylor and Francis: New York, 1987.

(29) Wang, W.; Schuchman, M. N.; Knolle, H. P.; von Sonntag, W. J.; von Sonntag, C. *J. Am. Chem. Soc.* **1999**, *121*, 238.

(30) Mishra, B. R.; Maity, D. K.; Priyadarsini, K. I.; Mohan, H.; Mittal, J. P. *J. Phys. Chem.* **2004**, *108*, 1552−1559.